

RENORM Predictions of Diffraction at LHC Confirmed

Konstantin Goulios

The Rockefeller University, 1230 York Avenue, New York, NY 10065, USA

Abstract. The RENORM model predictions of diffractive, total, and total-inelastic cross sections at the LHC are confirmed by recent measurements. The predictions of several other available models are discussed, highlighting their differences from RENORM, mainly arising from the way rapidity gap formation, low- and high-mass diffraction, unitarization, and hadronization are implemented.

Keywords: diffraction, pomeron, total cross section

PACS: 13.85.Lg, 13.85.Dz, 13.87.Cc, 12.40.Nn

In the CDF studies of diffraction at the Tevatron, all processes are well modeled by the MBR (Minimum Bias Rockefeller) Monte Carlo MC simulation, which is a stand-alone simulation based on the unitarized Regge-theory model RENORM [1], employing inclusive nucleon parton distribution functions (PDFs) and QCD color factors. An update of RENORM, first presented at EDS-2009 [2], includes a unique unitarization prescription for predicting the total pp cross section at high energies. This model has been included as an MBR option for simulating diffractive processes in PYTHIA8 since version PYTHIA8.165 [3], and will be referred to here-forth as PYTHIA8-MBR.

We discuss the following diffractive processes:

$$\begin{aligned} \text{SD} \quad pp \rightarrow Xp \\ \text{or} \quad pp \rightarrow pY \quad \text{Single Diffraction (or Single Dissociation),} \end{aligned} \quad (1)$$

$$\text{DD} \quad pp \rightarrow XY \quad \text{Double Diffraction (or Double Dissociation).} \quad (2)$$

The RENORM predictions are expressed as unitarized Regge-theory formulas, with unitarization achieved by a renormalization scheme in which the Pomeron (P) flux is interpreted as the probability for forming a diffractive (non-exponentially suppressed) rapidity gap, and thereby its integral over all phase space saturates when it reaches unity. Differential cross sections are expressed in terms of the P -trajectory $\alpha(t) = 1 + \varepsilon + \alpha' t$ with $\varepsilon = 0.104$ and $\alpha' = 0.25 \text{ GeV}^{-2}$, the P - p coupling $\beta(t)$, and the ratio of the triple- P to the P - p couplings, $\kappa \equiv g(t)/\beta(0)$. For large rapidity gaps, $\Delta y \geq 3$, for which P -exchange dominates, the cross sections are

$$\frac{d^2\sigma_{SD}}{dt d\Delta y} = \frac{1}{N_{\text{gap}}(s)} \left[\frac{\beta^2(t)}{16\pi} e^{2[\alpha(t)-1]\Delta y} \right] \cdot \left\{ \kappa\beta^2(0) \left(\frac{s'}{s_0} \right)^\varepsilon \right\}, \quad (3)$$

$$\frac{d^3\sigma_{DD}}{dt d\Delta y dy_0} = \frac{1}{N_{\text{gap}}(s)} \left[\frac{\kappa\beta^2(0)}{16\pi} e^{2[\alpha(t)-1]\Delta y} \right] \cdot \left\{ \kappa\beta^2(0) \left(\frac{s'}{s_0} \right)^\varepsilon \right\}, \quad (4)$$

where t is the 4-momentum-transfer squared at the proton vertex, Δy the rapidity-gap width, and y_0 the center of the rapidity gap.

The total cross section σ_{tot} is expressed as [4]

$$\sigma_{\text{tot}}^{p^+p} = 16.79s^{0.104} + 60.81s^{-0.32} \mp 31.68s^{-0.54} \quad \text{for } \sqrt{s} \leq 1.8 \text{ TeV}, \quad (5)$$

$$\sigma_{\text{tot}}^{p^+p} = \sigma_{\text{tot}}^{\text{CDF}} + \frac{\pi}{s_0} \left[\left(\ln \frac{s}{s_F} \right)^2 - \left(\ln \frac{s^{\text{CDF}}}{s_F} \right)^2 \right] \quad \text{for } \sqrt{s} \geq 1.8 \text{ TeV}, \quad (6)$$

where p^+ (p^-) stands for p (\bar{p}), and s_0 (s_F) are scaling parameters, interpreted as the collision energy squared (Pomeron flux) saturation scales. For $\sqrt{s} \leq 1.8 \text{ TeV}$, where there are Reggeon contributions, we use the global-fit expression [5], while for $\sqrt{s} \geq 1.8 \text{ TeV}$, where Reggeon contributions are negligible, we employ the Froissart-Martin formula [6, 7, 8]. The two expressions are smoothly matched at $\sqrt{s} \approx 1.8 \text{ TeV}$.

The elastic cross section for $\sqrt{s} \leq 1.8 \text{ TeV}$ is obtained from the global fit [5], while for $1.8 < \sqrt{s} \leq 50 \text{ TeV}$ we use an extrapolation of the global-fit ratio of $\sigma_{\text{el}}/\sigma_{\text{tot}}$, which is slowly varying with \sqrt{s} , multiplied by σ_{tot} . The total non-diffractive cross section is then calculated as $\sigma_{\text{ND}} = (\sigma_{\text{tot}} - \sigma_{\text{el}}) - (2\sigma_{\text{SD}} + \sigma_{\text{DD}} + \sigma_{\text{CD}})$.

Figure 1 (left) shows the TOTEM total, elastic, and total-inelastic cross sections, along with results from other experiments, fitted by the COMPETE Collaboration [9]. The RENORM predictions, displayed as filled (green) squares, are in excellent agreement with the TOTEM results. Similarly, in Fig. 1 (right), good agreement is observed between inelastic cross-section measurements at $\sqrt{s} = 7$ TeV and the corresponding PYTHIA8-MBR predictions [11].

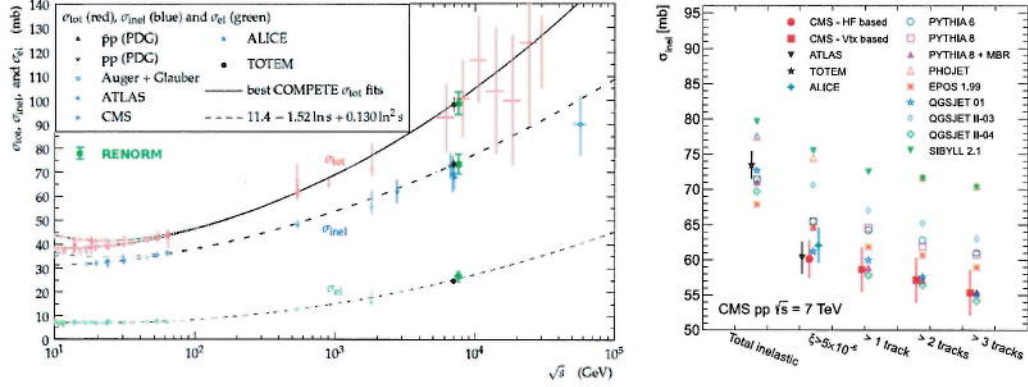


FIGURE 1. (left) TOTEM measurements of the total, total-inelastic, and elastic pp cross sections at $\sqrt{s} = 7$ TeV, shown with best COMPETE fits [9] and RENORM predictions; (right) inelastic cross-section measurements at $\sqrt{s} = 7$ TeV are in good agreement with RENORM / PYTHIA8-MBR predictions [11]).

Another example of the predictive power of RENORM is shown in Fig. 2, which displays the total SD (left) and DD (right) cross sections from various experiments for $\xi < 0.05$. The point labeled KG* was obtained by extrapolating into the low mass region the measured CMS cross sections at higher mass regions (see Ref. [12]) using RENORM. The curves represent the theoretical predictions embedded in the models displayed in the RHS inset: PYTHIA8-MBR with $\epsilon = 0.104$ or $\epsilon = 0.08$, GLM (E. Gotsman, E. Levin, and E. U. Maor) [13], and KP (A. B. Kaidalov and M. G. Poghosyan) [14].

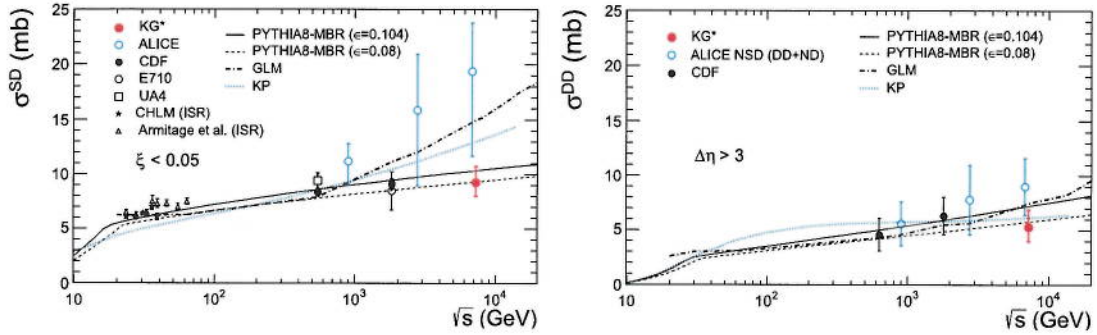


FIGURE 2. Measured SD (left) and DD (right) cross sections for $\xi < 0.05$ compared with theoretical predictions. The KG* point was obtained from the measured CMS cross sections [12] by extrapolation into the unmeasured low mass region(s) using the MBR model embedded in PYTHIA8-MBR.

Figure 3 shows the $\xi_x = M_x^2/s$ dependence of the SD cross section for the PYTHIA8-4C, PYTHIA6-D6T, PHOJET [15, 16], QGSJET-II-03(LHC) [17], QGSJET-II-04(LHC) [17], and EPOS-LHC [18] simulations, compared to the nominal PYTHIA8-MBR simulation, for two regions of ξ_x : $-5.5 < \log_{10} \xi_x < -2.5$ (yellow) and $\xi_x < 0.05$ (khaki). The PYTHIA8-MBR predictions with values of α' and ϵ changed to $\alpha' = 0.125 \text{ GeV}^{-2}$, $\epsilon = 0.104$, and $\epsilon = 0.07$ (one parameter changed at a time) are also included in order to provide a scale for their effect on the cross sections.

We note that:

- The models PYTHIA8-4C, PYTHIA6-D6T, and PHOJET do not predict correctly the ξ_x dependence of the SD cross section, while QGSJET-II-04(LHC) and EPOS-LHC underestimate it in the region of the CMS measurement.
- The RENORM/NBR model describes well the SD and DD measurements, both in shape and normalization.
- As shown in Fig. 1, RENORM/NBR also describes well the measured total, elastic, and total inelastic cross sections.

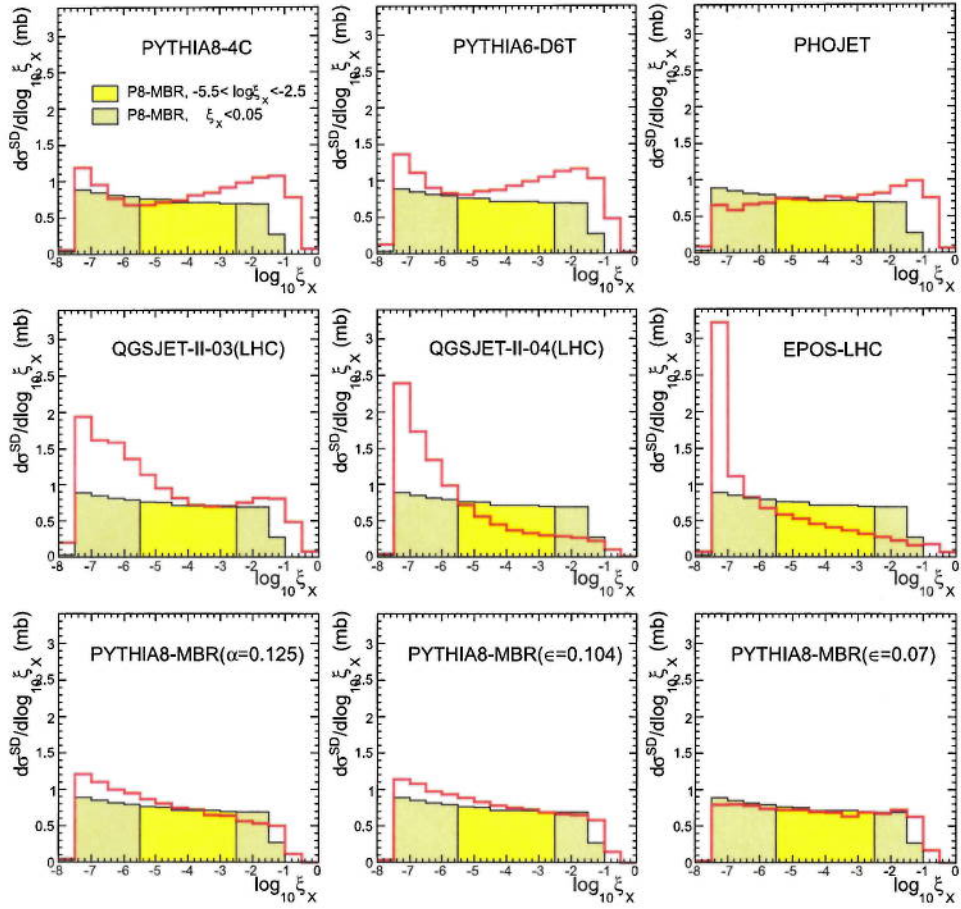


FIGURE 3. The generator-level SD cross section as a function of $\xi_X = M_X^2/s$, shown for PYTHIA8-4C, PYTHIA6-D6T, PHOJET, QGSJET-II-03(LHC), QGSJET-II-04(LHC), EPOS-LHC, and PYTHIA8-MBR with the parameters of Pomeron trajectory changed from the nominal values ($\alpha' = 0.25 \text{ GeV}^{-2}$, $\epsilon = 0.08$) to $\alpha' = 0.125 \text{ GeV}^{-2}$, $\epsilon = 0.104$, and $\epsilon = 0.07$ (one parameter changed at a time). The nominal PYTHIA8-MBR simulation is presented in each plot for the regions of ξ_X , $-5.5 < \log_{10} \xi_X < -2.5$ (yellow) and $\xi_X < 0.05$ (khaki), from which the measured SD cross section is extrapolated (from yellow to khaki).

The above findings fully justify using RENORM for the extrapolation of the measured SD and DD cross sections to the regions where there is no detector coverage.

In summary, we compare our pre-LHC predictions for the total, elastic, total-inelastic, and single/double diffractive components of the pp cross sections LHC, based on the RENORM/NBR model, with recent LHC data and other-model predictions, namely PYTHIA8-4C, PYTHIA6-D6T, PHOJET, QGSJET-II-03(LHC), QGSJET-II-04(LHC), EPOS-LHC, and PYTHIA8-MBR. The RENORM/NBR predictions are confirmed as best describing simultaneously all aspects of the data.

ACKNOWLEDGMENTS

I would like to thank Dr. Robert Adam Ciesielski, my colleague at Rockefeller and collaborator in the implementation of the MBR simulation into PYTHIA8, and the Office of Science of the Department of Energy for supporting the Rockefeller experimental diffraction physics programs at Fermilab and LHC on which this research is encored.

REFERENCES

1. K. Goulianos, "Hadronic Diffraction: Where do we Stand?", in *Les Rencontres de Physique de la Vallée d'Aoste: Results and Perspectives in Particle Physics*, La Thuile, Italy (2004), Frascati Physics Series, Special 34 Issue, Ed. Mario Greco [arXiv:hep-ph/0407035].
2. K. Goulianos, "Diffractive and Total pp Cross Sections at LHC", in *13th International Conference on Elastic and Diffractive Scattering (Blois Workshop) - Moving Forward into the LHC Era* [arXiv:1002.3527v2].
3. T. Sjöstrand, S. Mrenna and P. Skands, in "JHEP05, 026 (2006)", *Comput. Phys. Comm.* 178 852 (2008) [arXiv:hep-ph/0603175, arXiv:0710.3820].
4. R. Ciesielski and K. Goulianos, "NBR Monte Carlo Simulation in PYTHIA8 (2012)" [arXiv:1205.1446].
5. R. J. M. Covolan, J. Montanha and K. Goulianos, *Phys. Lett. B* **389**, 176 (1996).
6. M. Froissart, *Phys. Rev.* **3**, 123 (1961).
7. A. Martin, *Nuovo Cimento* **42**, 930 (1966).
8. A. Martin, *Phys. Rev. D* **80**, 065013 (2009).
9. M. Deile (TOTEM Collaboration), "Measurements of Proton-Proton and Total Cross Section at the LHC by TOTEM", in *Diffraction 2012*, *AIP Conf. Proc.* 1523, 314 (2013) [doi:http://dx.doi.org/10.1063/1.4802175].
10. B. Abelev et al. (ALICE Collaboration), *Eur. Phys. J. C* (2013)73:2456 [arXiv:1208.4968, DOI 10.1140/cpjc/s10052-013-2456-0].
11. S. Chatrchyan et al. (CMS Collaboration), *Phys. Lett. B* **722**, 5 (2013).
12. R. A. Ciesielski, "Measurements of diffraction in p-p collisions in CMS", in *XXI International Workshop on Deep-Inelastic Scattering and Related Subjects* [PoS(DIS 2013)091].
13. E. Gotsman, E. Levin, and E. U. Maor, "Description of LHC data in a soft interaction model," *Phys. Lett. B* **16**,425 (2012) [doi:10.1016/j.physletb.2012.08.042, arXiv:1208.0898].
14. A. B. Kaidalov and M. G. Poghosyan, "Predictions of proton-proton interaction cross-sections at LHC" [arXiv:1109.3697].
15. F. W. Bopp, R. Angel, and J. Ranft, "Rapidity gaps in the PHOJET Monte Carlo" [arXiv:hep-ph/9803437].
16. R. Angel, *Z. Phys. C* **66**, 203 (1995) [doi:10.1007/BF01496594].
17. S. Ostapchenko, "QGSJET-II: physics, recent improvements, and results for air showers", *EPJ Web of Conferences* **52**, 02001 (2013) [http://dx.doi.org/10.1051/epjconf/20125202001].
18. T. Pierog, Iu. Karpenko, J.M. Katzy, E. Yatsenko, K. Werner, "EPOS LHC: test of collective hadronization with LHC data" [http://arxiv.org/abs/1306.0121].
19. K. Goulianos, "Predictions of Diffractive Cross Sections in Proton-Proton Collisions", in *Diffraction 2012, International Workshop on Diffraction in High Energy Physics*, *AIP Conf. Proc.* 1523, 107 (2013) [doi:http://dx.doi.org/10.1063/1.4802128].